Towards the Automatic Detection of Volcanic Unrest using Sentinel-1 InSAR data and Machine Learning

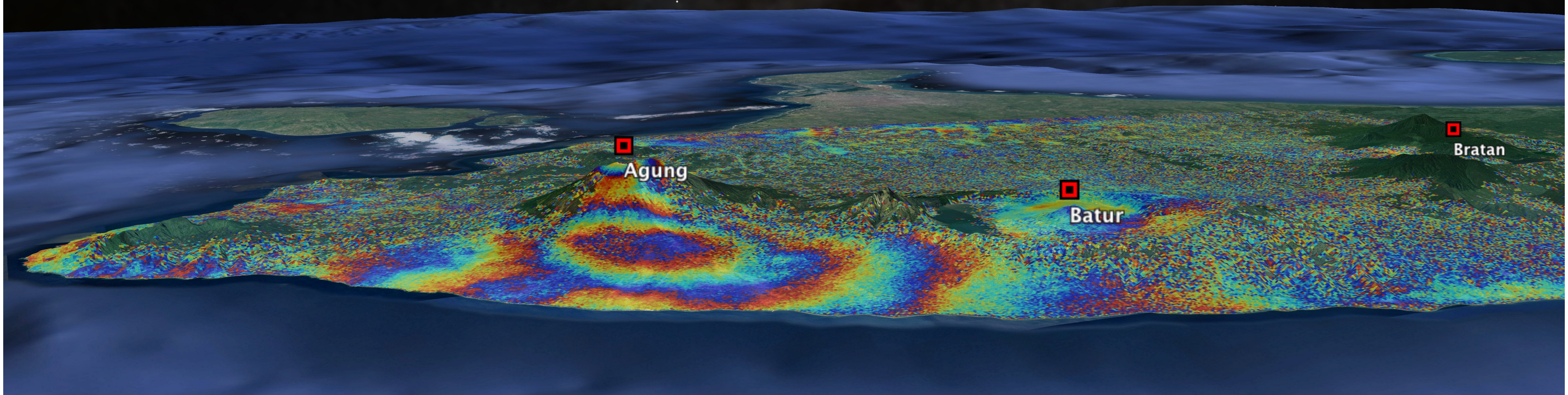

Juliet Biggs, Nantheera Anantrasirichai, Fabien Albino and David Bull

University of BRISTOL
COMET
VILab
Visual Information Laboratory

Global InSAR Databases

1) A significant statistical link to volcanic eruptions :

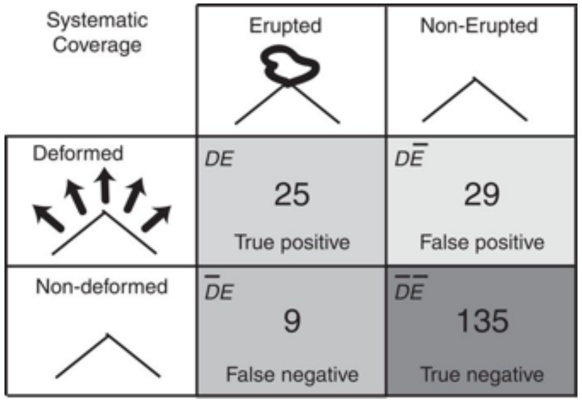

2) InSAR detections often pre-eruptive (~50%):

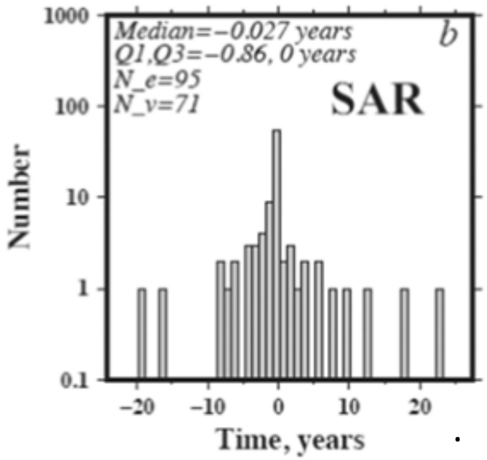

3) Architecture of active magmatic systems:

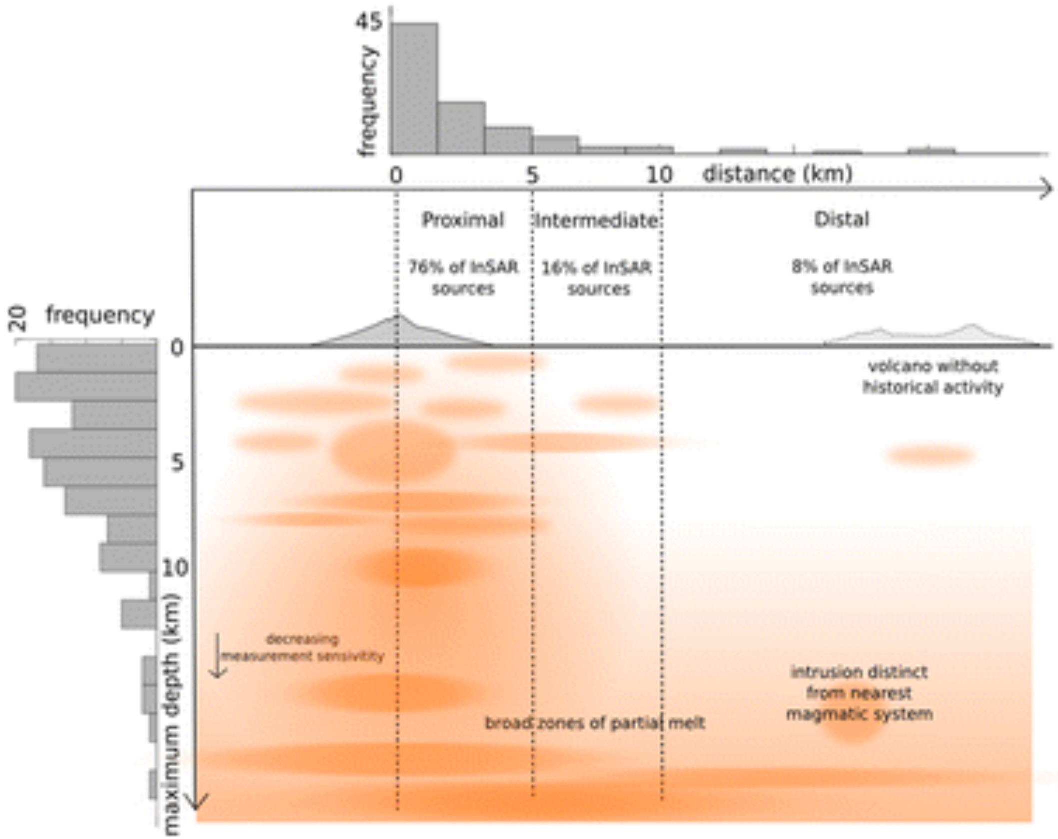

Biggs et al, 2014, Furtney et al, 2018, Ebmeier et al, 2018

Global Volcano Monitoring: The LïCSAR-volcano database

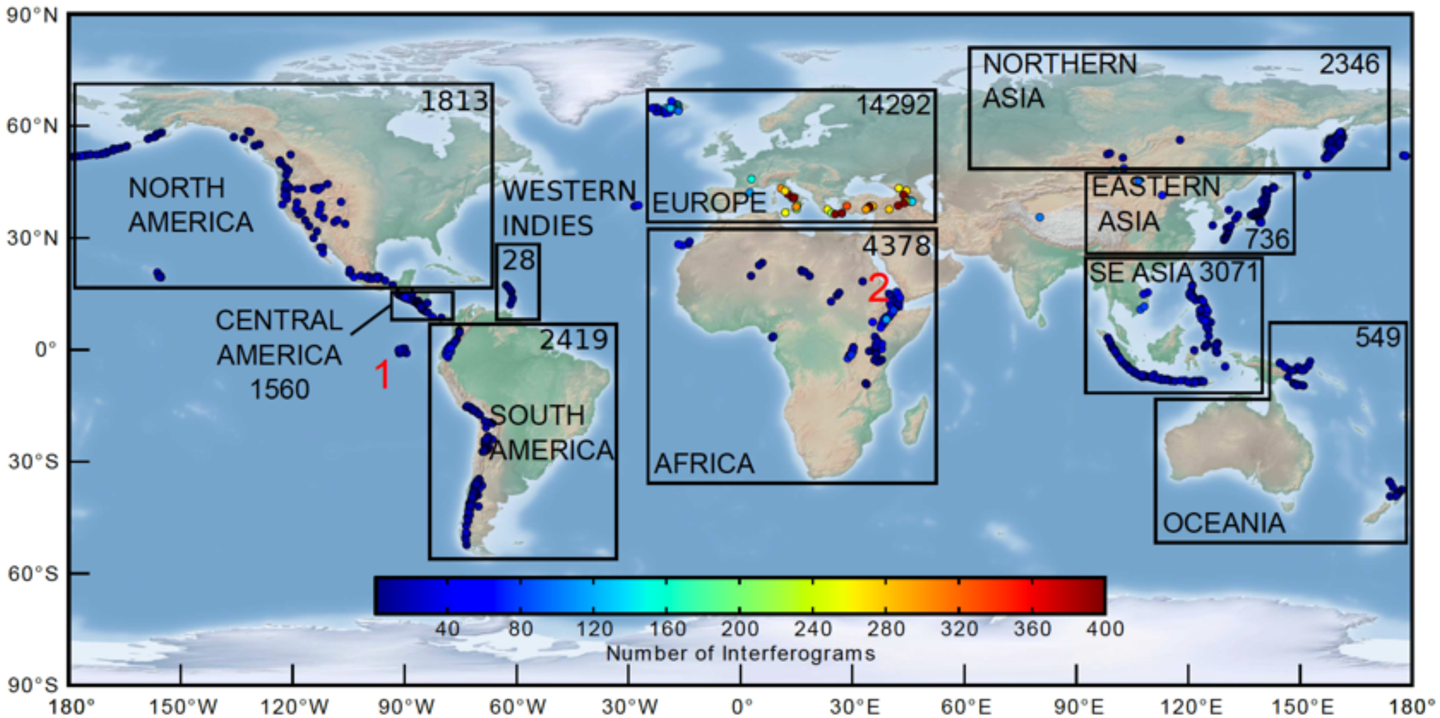

- Sentinel-1 generates >10-TB data per day
- The explosion in data has brought major challenges associated with timely dissemination of information.

- Test dataset of ~30,000 interferograms at >900 active volcanoes produced by LiCSAR
- Now up to >200,000 (October 2019).
- Anticipate 1 million images per year when fully operational.

http://comet.nerc.ac.uk/ COMET-LiCS-portal/).

Automated Processing: The LïCSAR-volcano database

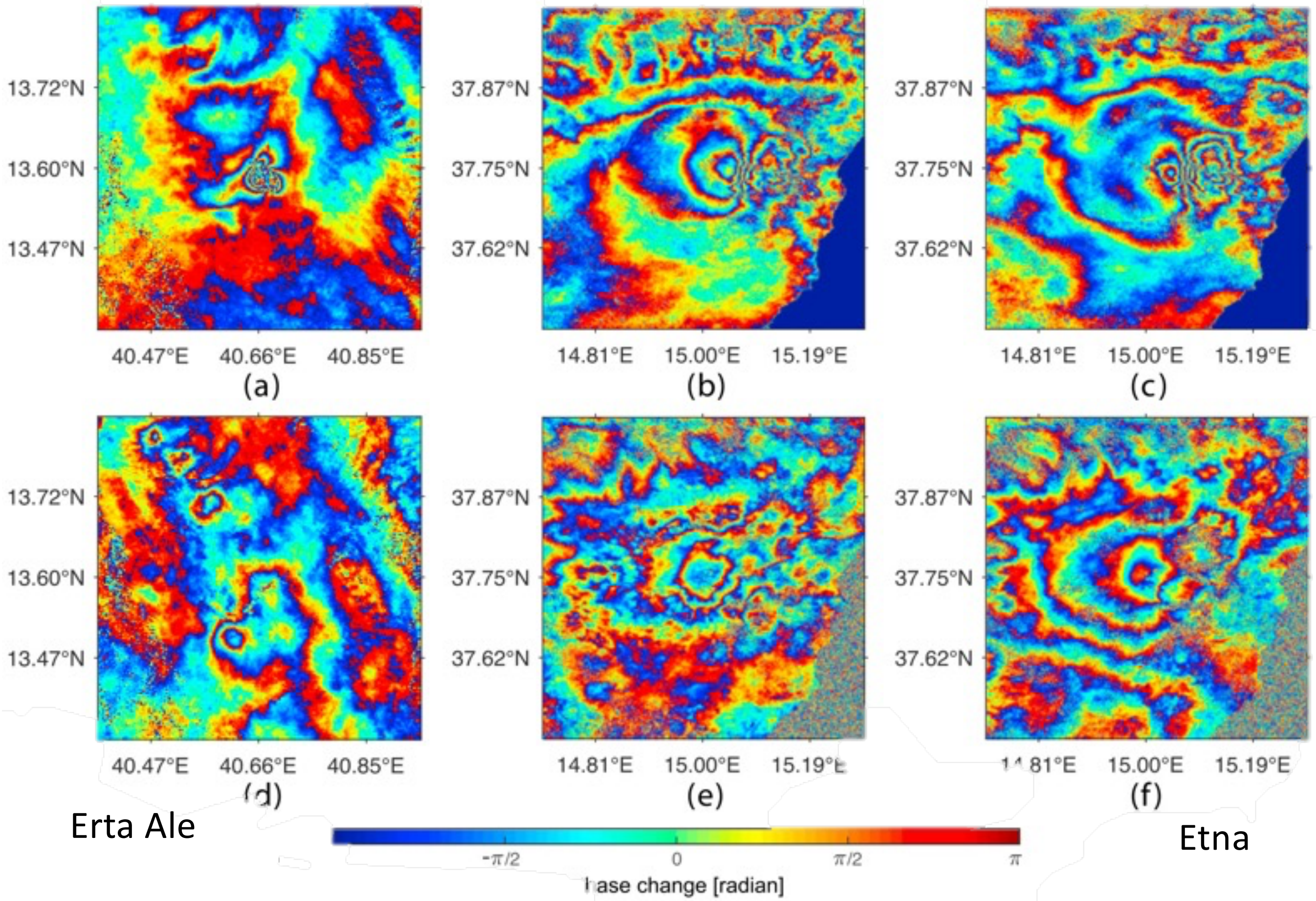

Ground deformation, background, noise or atmosphere?

Image Classification with Machine Learning

Feature extraction

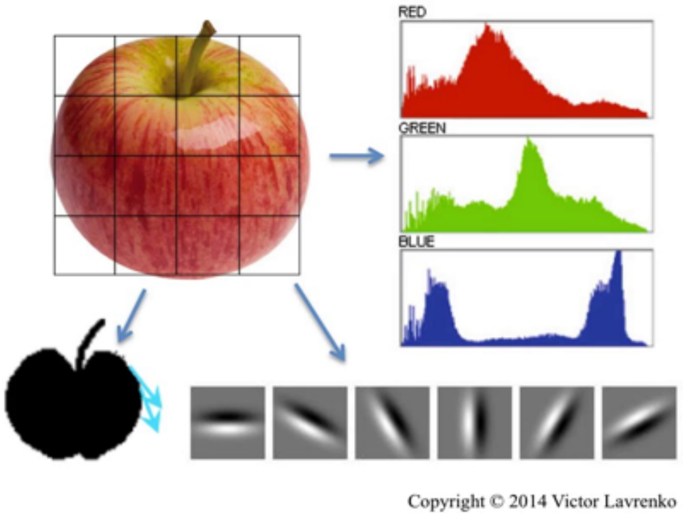

Classification

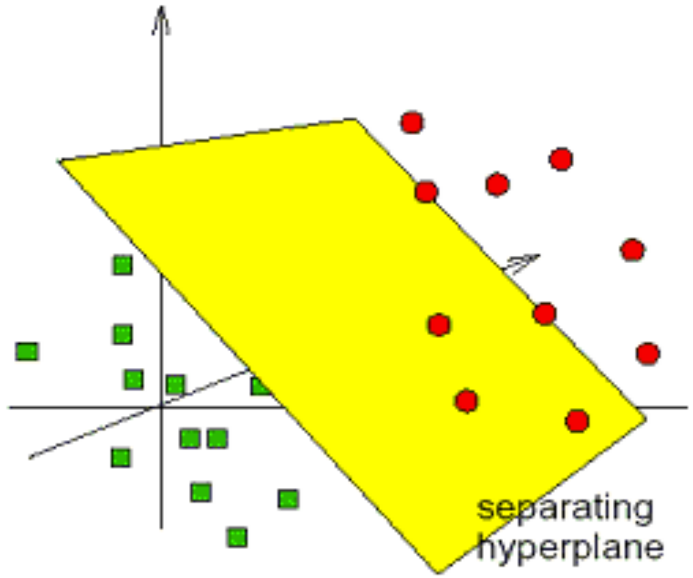

Deep learning → Feature extraction and modelling steps are automatic.

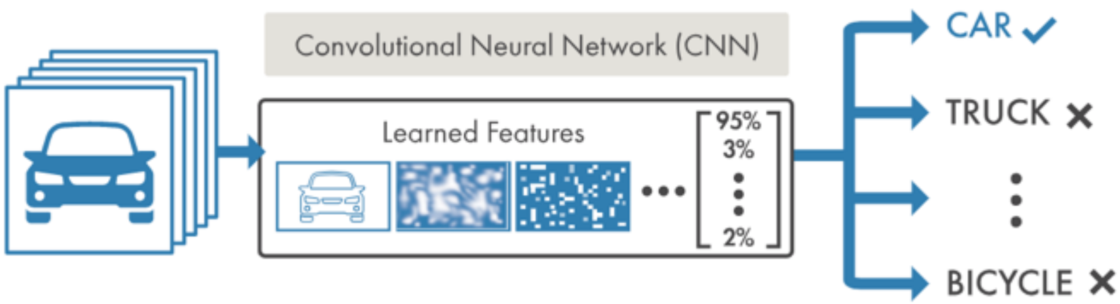

Proposed framework

Training Process

Prediction Process

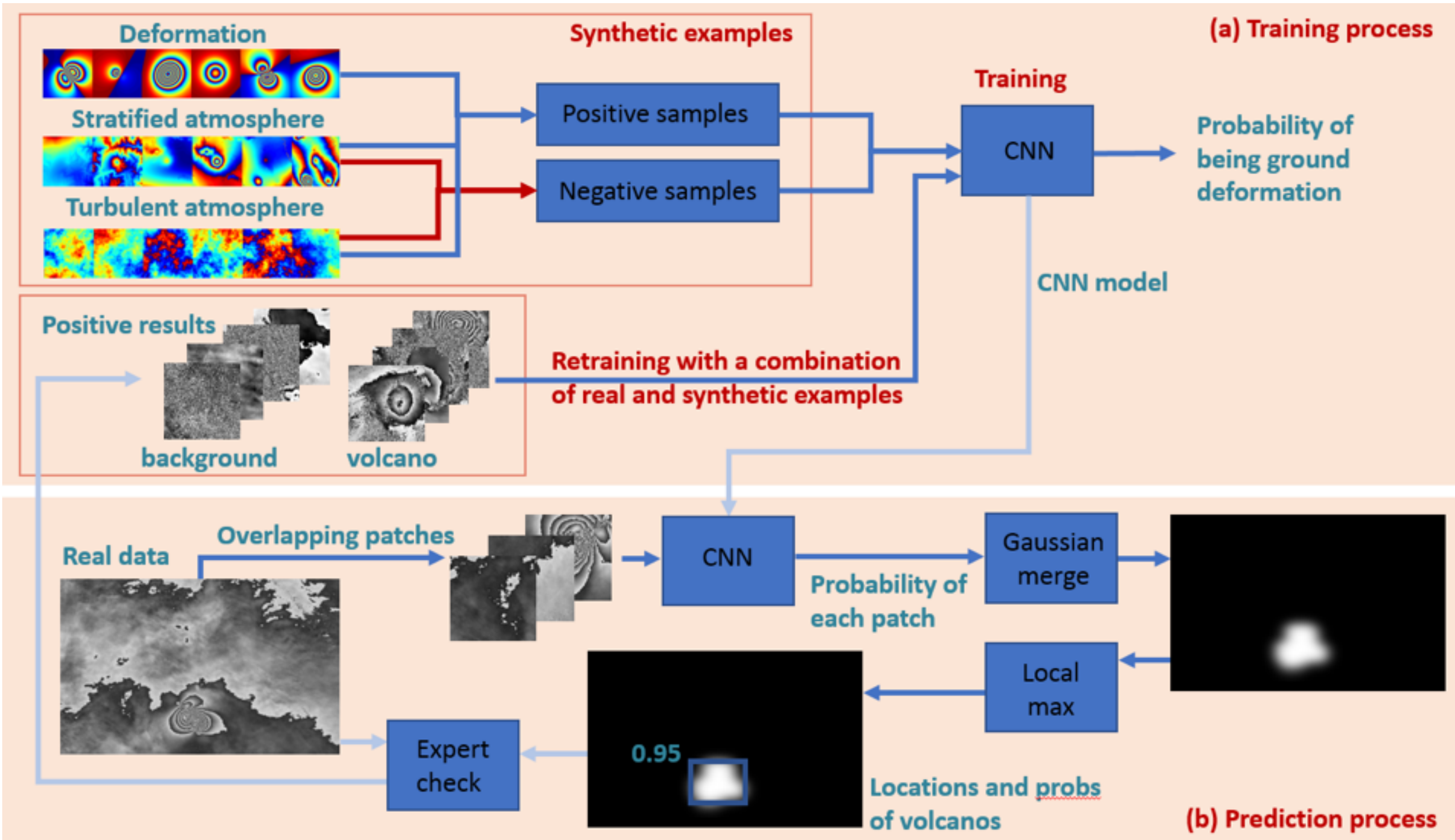

Training Dataset 1: Envisat Data

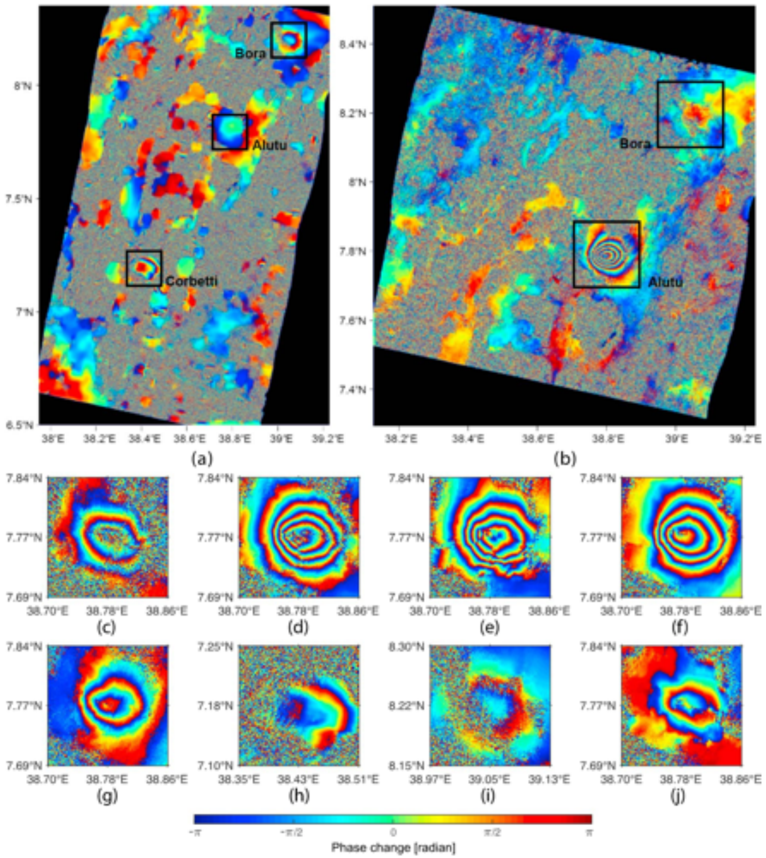

Envisat Dataset

Volcano name	Type	Period	# of interferograms
Alutu	Stratovolcano	2003–2010	158
Bora	Pyroclastic cone	2003–2010	52
Corbetti	Caldera	2003–2010	44
Haledebi	Fissure vent	2003–2010	46

Data augmentation: rotations, flips, distortions, and pixel shifts.

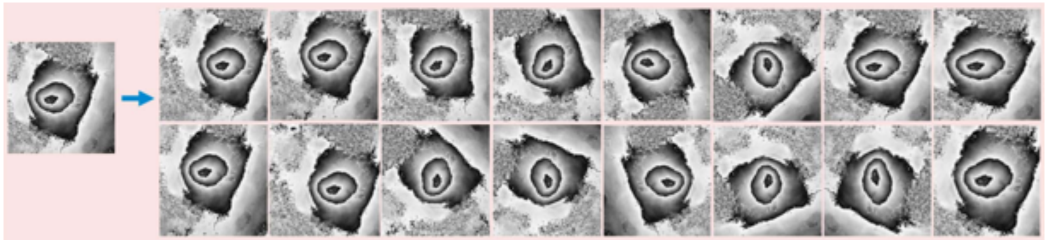

300 positive samples → 10,000 positive samples

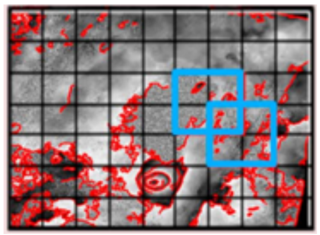

Edge detection to reduce negative samples, then randomly select 10,000 of them.

Anantrasirichai et al, 2018, JGR

Training Dataset 2: Synthetic components

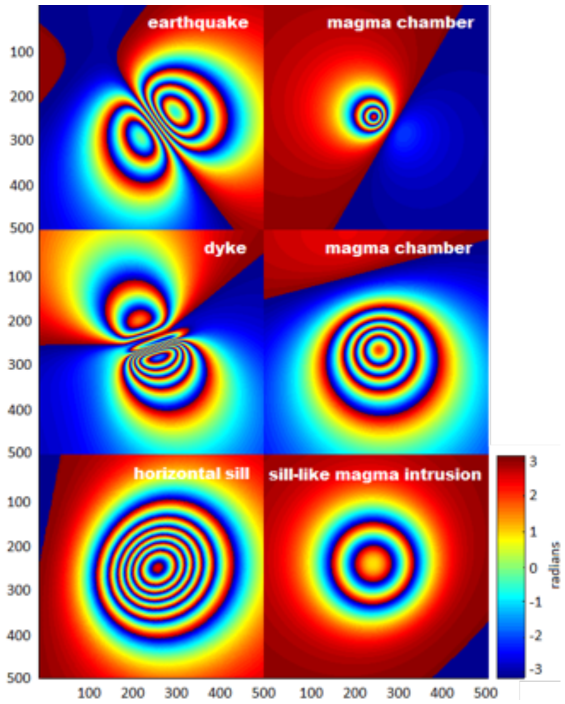

Deformation (D)

- Use a Monte Carlo approach to select source parameters and project the 3-D surface displacement into the satellite line-of-sight.
- Okada, Mogi, Fialko.

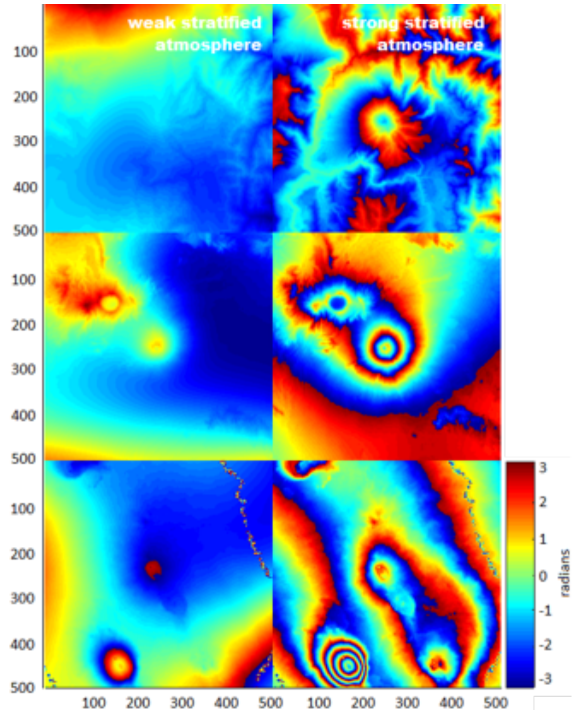

Stratified atmosphere (S)

- Generic Atmospheric Correction Online Service (GACOS)
- 100 GACOS tropospheric delay maps from each of 100 representative volcanoes with 12-day intervals.

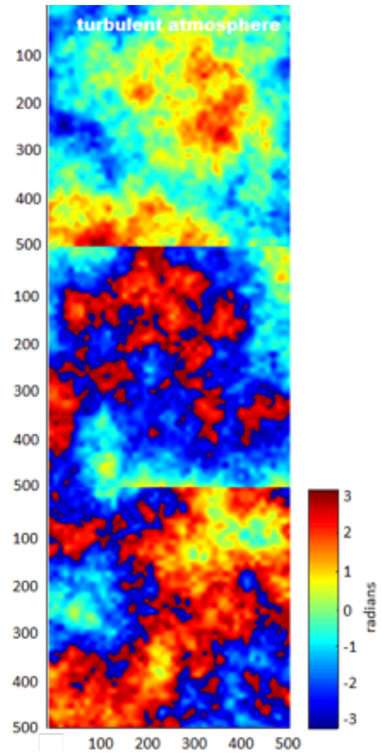

Turbulent atmosphere (T)

- Turbulent atmospheric delays are spatially correlated and their covariance can be described using an exponentially decaying function

Anantrasirichai et al, 2019, RSE

Training Dataset 2: Synthetic Interferograms

Stratified Atmosphere (S) only

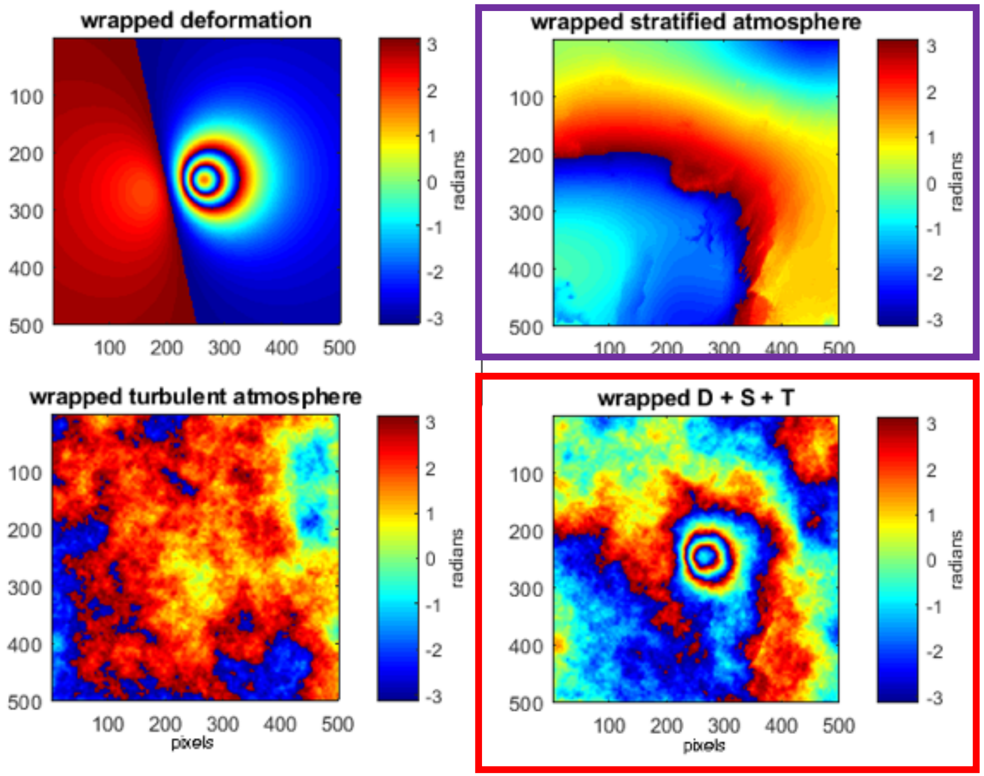

Final Interferogram

'Easy' Example:
(S from Aluto, Ethiopia)

Stratified Atmosphere (S) only

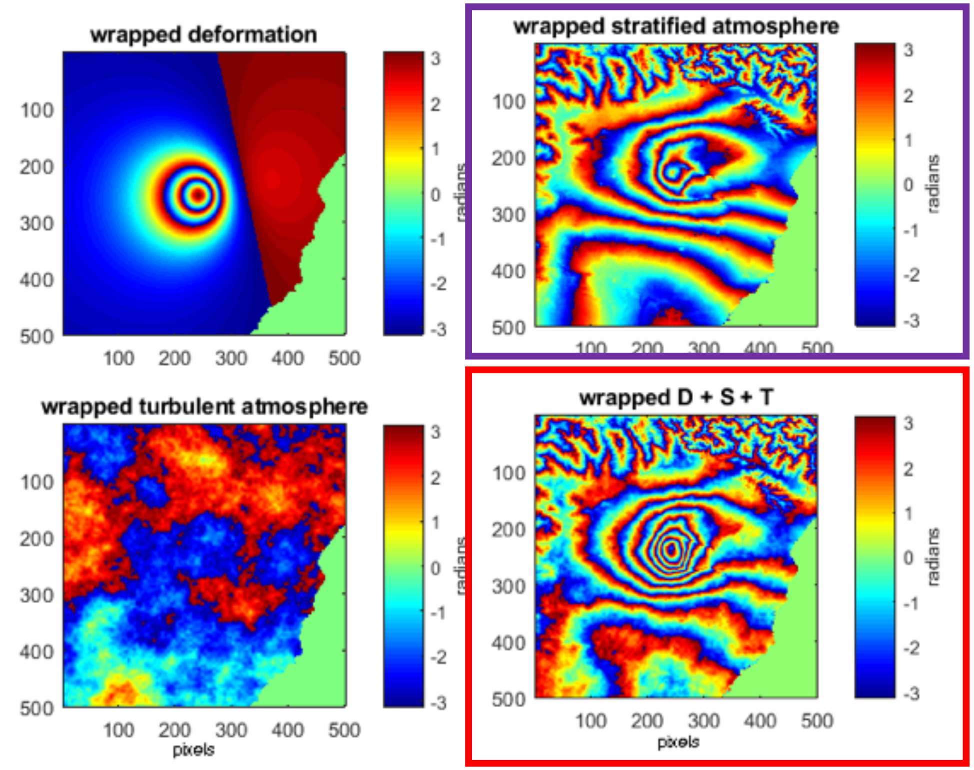

Final Interferogram

'Challenging' Example:
(S from Etna)

Anantrasirichai et al, 2019, RSE

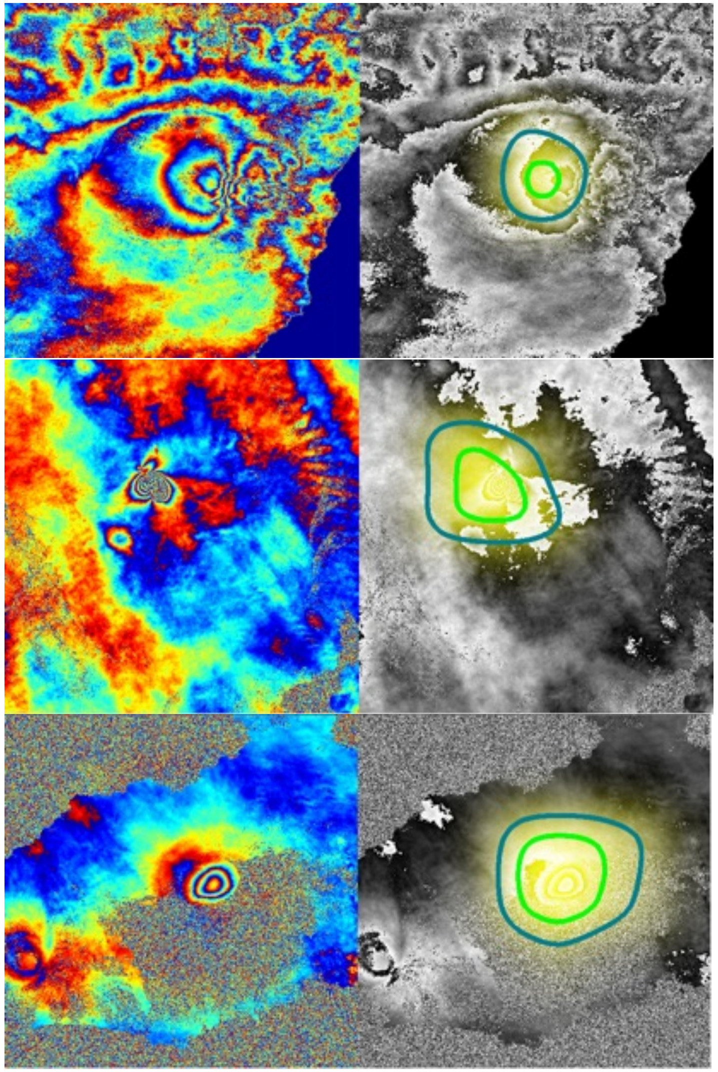

True Positives (TP)

Application to Real Data

30,249 interferograms in LicSAR test dataset

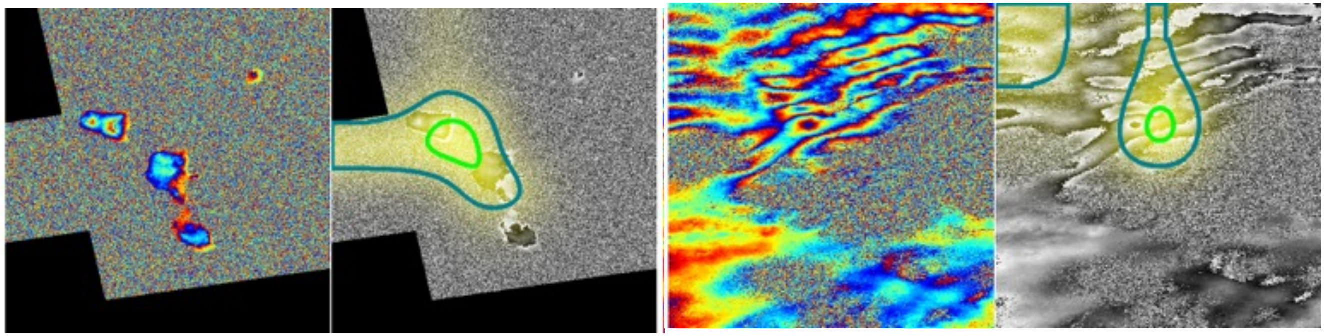

False Positives (FP)

Training Data	#P	#TP	#FP	#FN
Envisat	1369	42	1327	0
Synthetic aD+bS+cT	334	41	293	1

Application to Real Data

30,249 interferograms in LicSAR test dataset

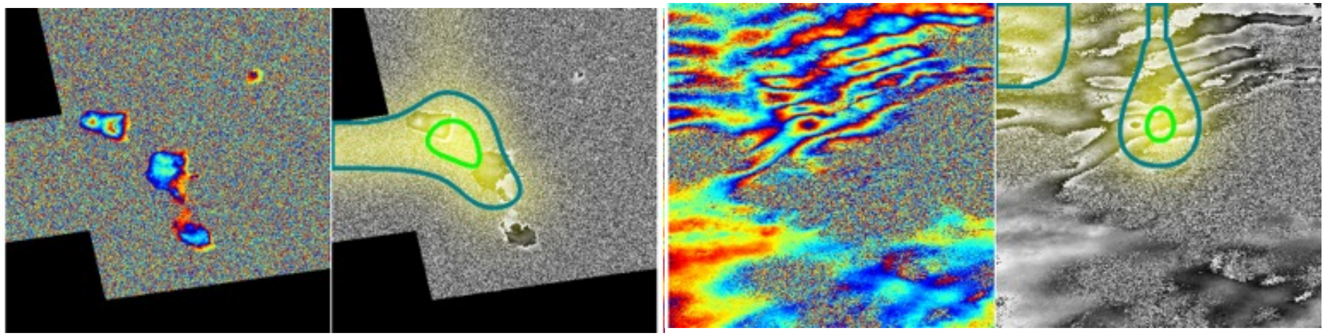

False Positives (FP)

Training Data	#P	#TP	#FP	#FN
Envisat	1369	42	1327	0
Synthetic aD+bS+cT	334	41	293	1
Envisat + FP	**104**	**42**	**62**	**0**
Synthetic + FP	**50**	**41**	**9**	**1**

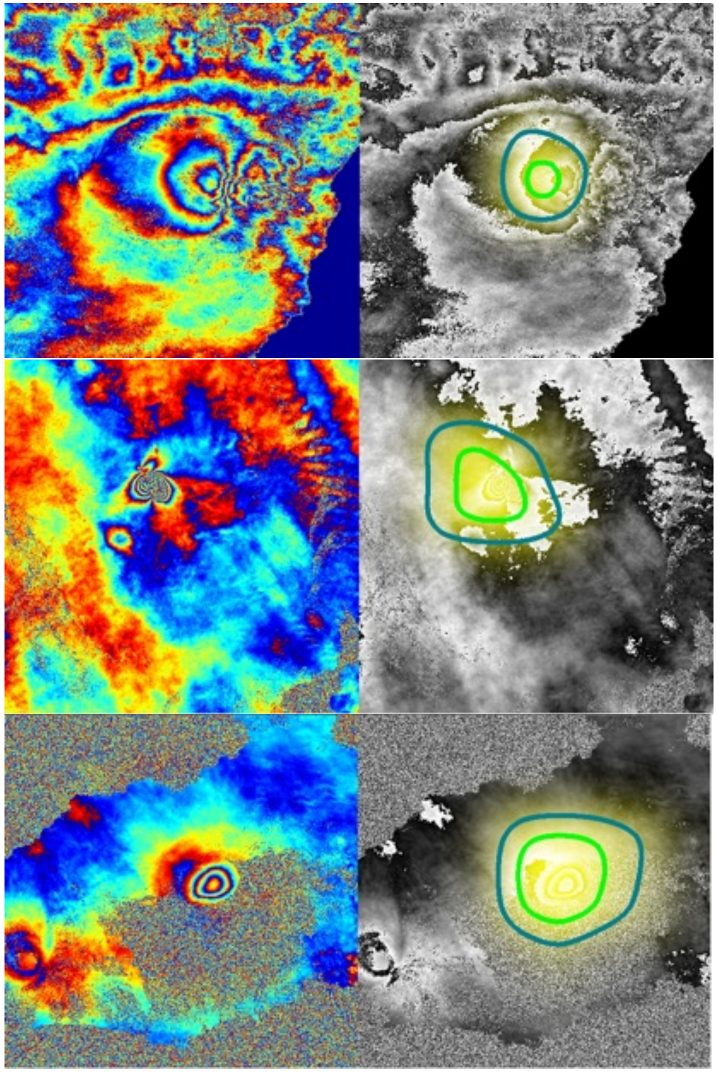

True Positives (TP)

Application to Real Data

30,249 interferograms in LicSAR test dataset

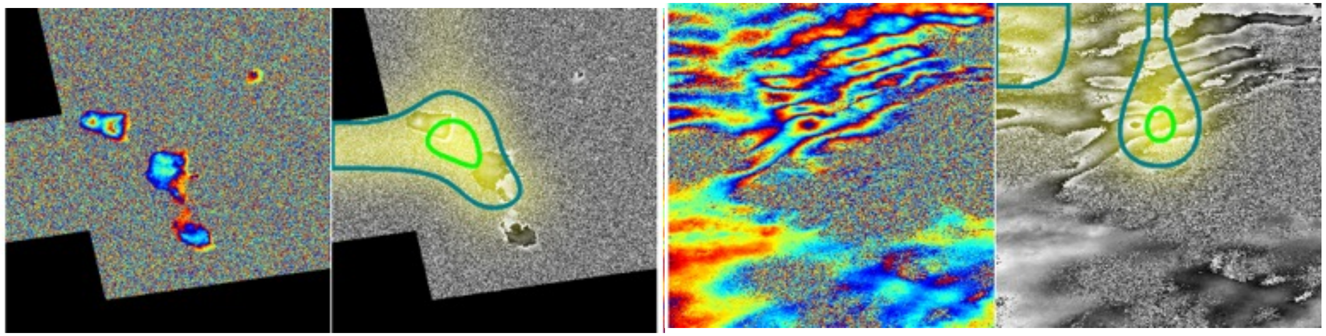

False Positives (FP)

Training Data	#P	#TP	#FP	#FN
Envisat	1369	42	1327	0
Synthetic aD+bS+cT	334	41	293	1
Envisat + FP	**104**	**42**	**62**	**0**
Synthetic + FP	**50**	**41**	**9**	**1**
--------------------------------	----------	------	--------	------
Synthetic + FP + GACOS	**41**	**41**	**0**	**1**

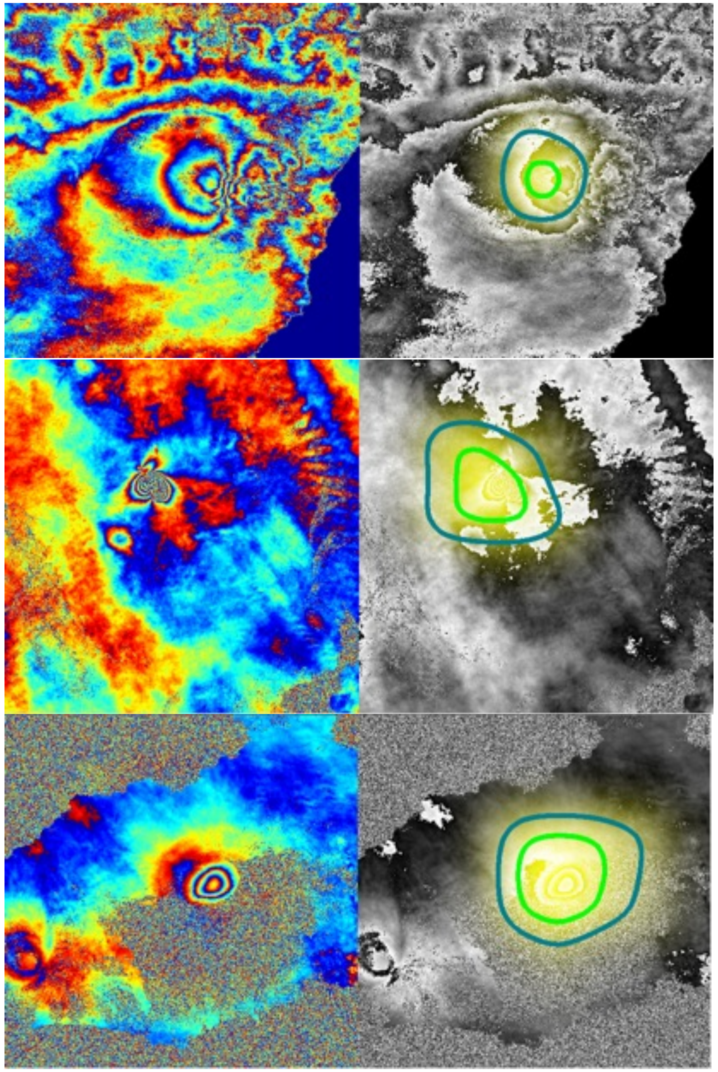

True Positives (TP)

False Negatives

- Current CNN trained to detect rapid deformation signals that produce multiple fringes in a single interferogram

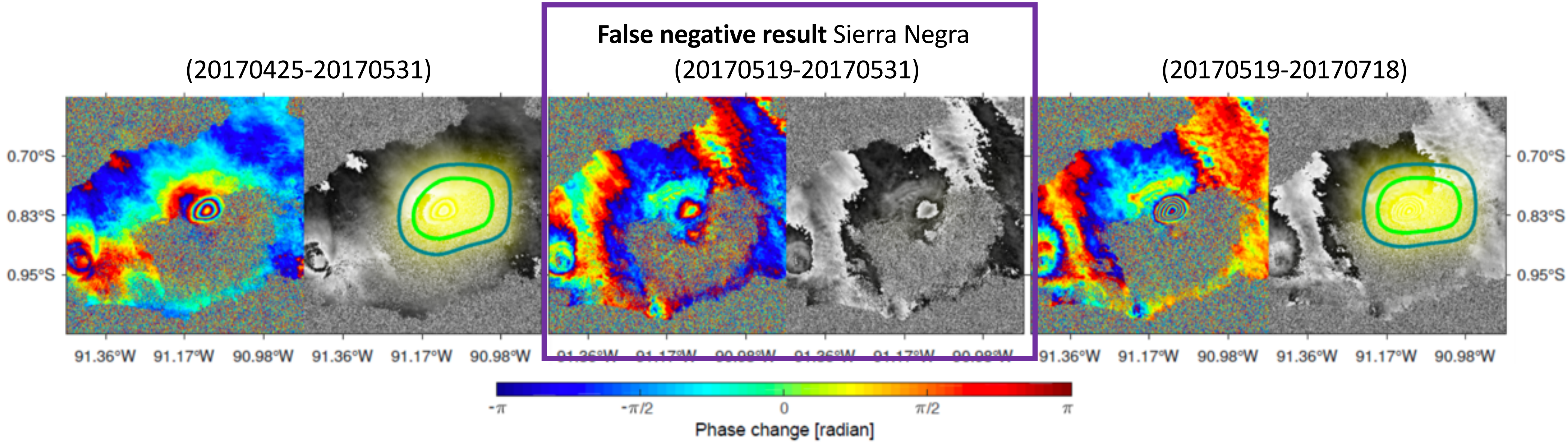

- Need a new training strategy/ dataset to detect **Slow Deformation**:
  - Stacked Interferograms
  - Wrapping Interval
  - Outlier Detection

Detecting Slow Deformation

- Slow, steady deformation is common.
- Can we improve detection thresholds?

1 fringe in a 12 day interferogram = 85 cmyr

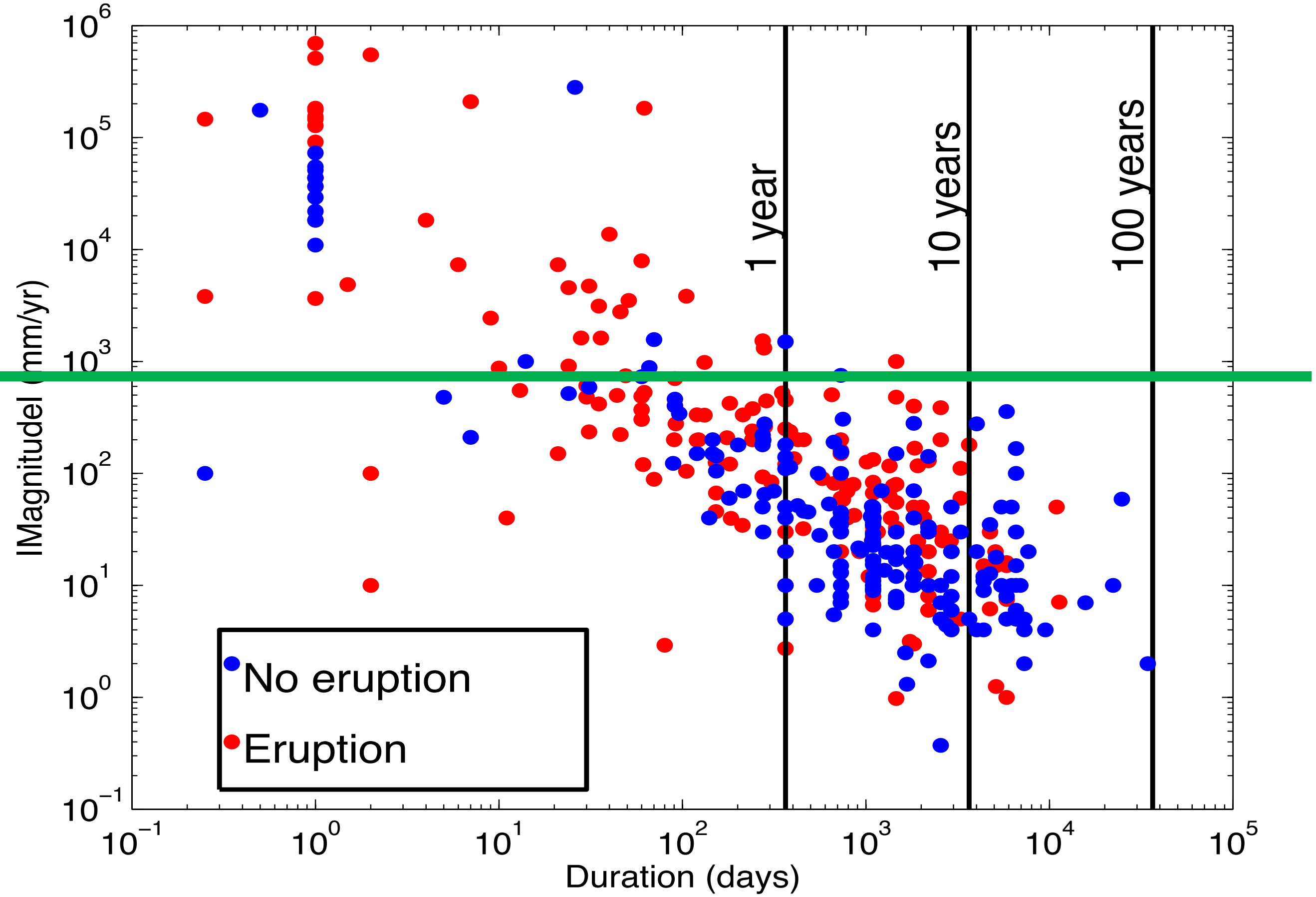

Biggs & Pritchard, 2017

Detection Thresholds: Synthetic Data

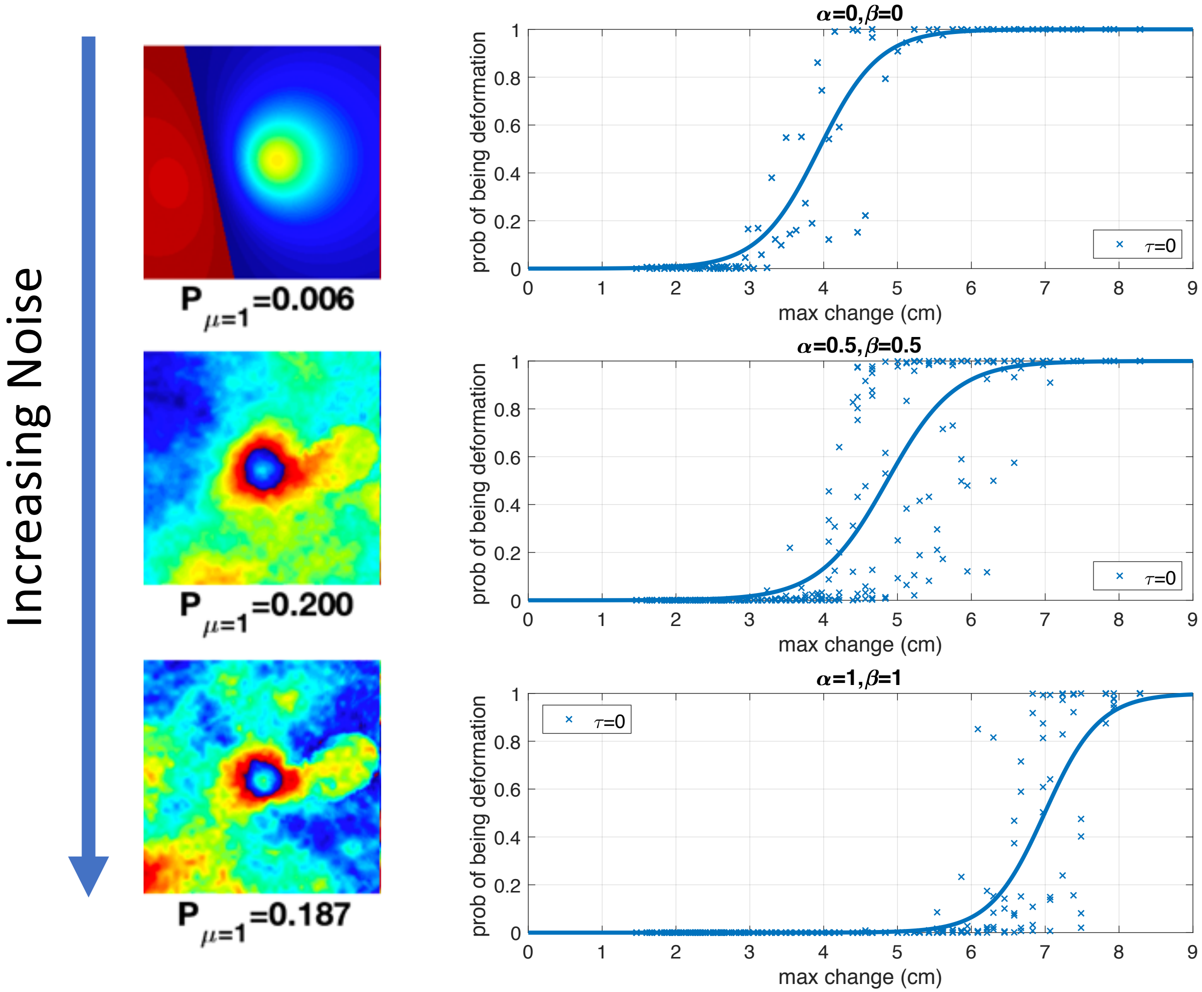

Anantrasirichai et al, in press

Synthetic Data

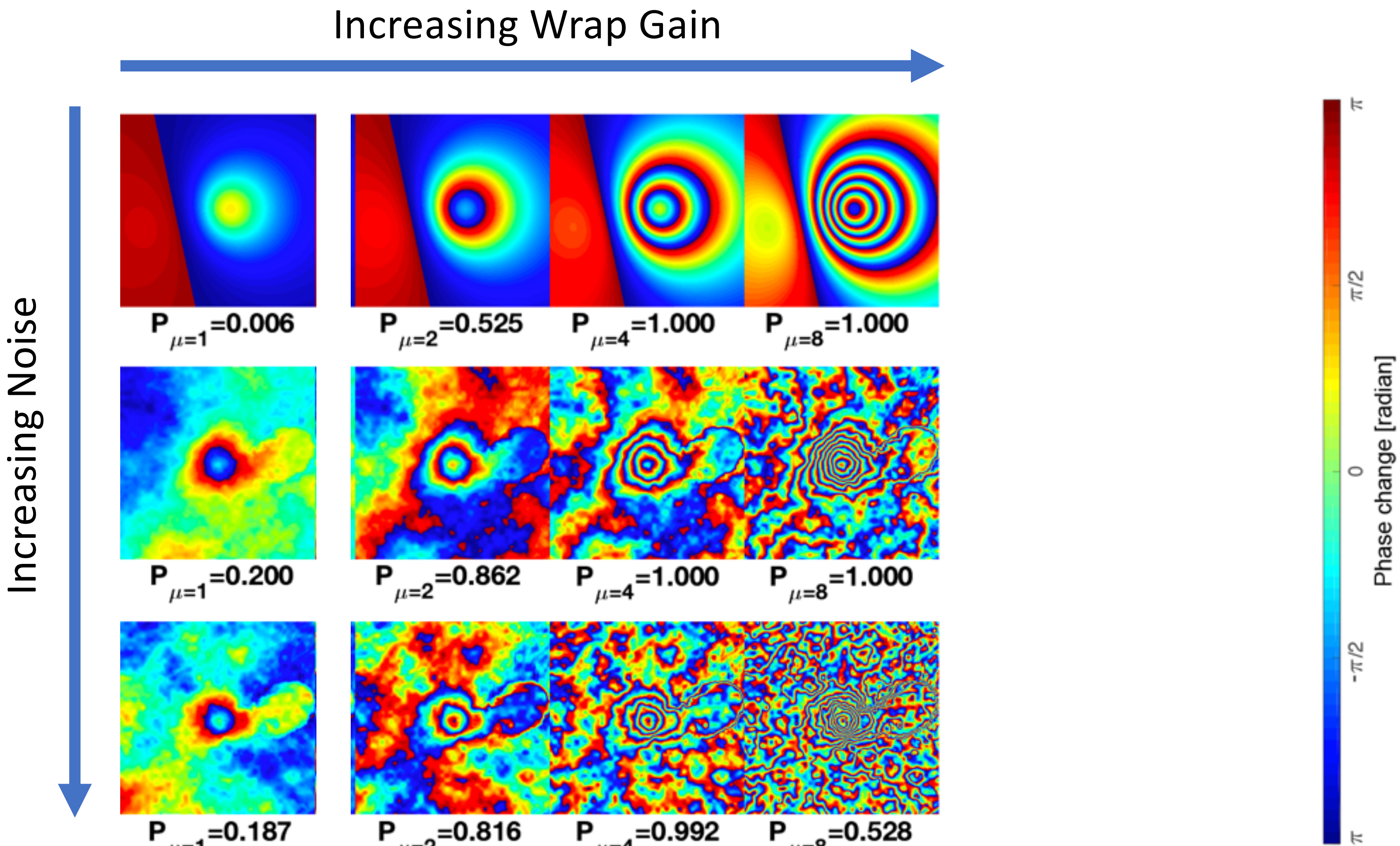

Anantrasirichai et al, in press

Detection Thresholds: Synthetic Data

Increase wrapping ($\boldsymbol{\mu}$)

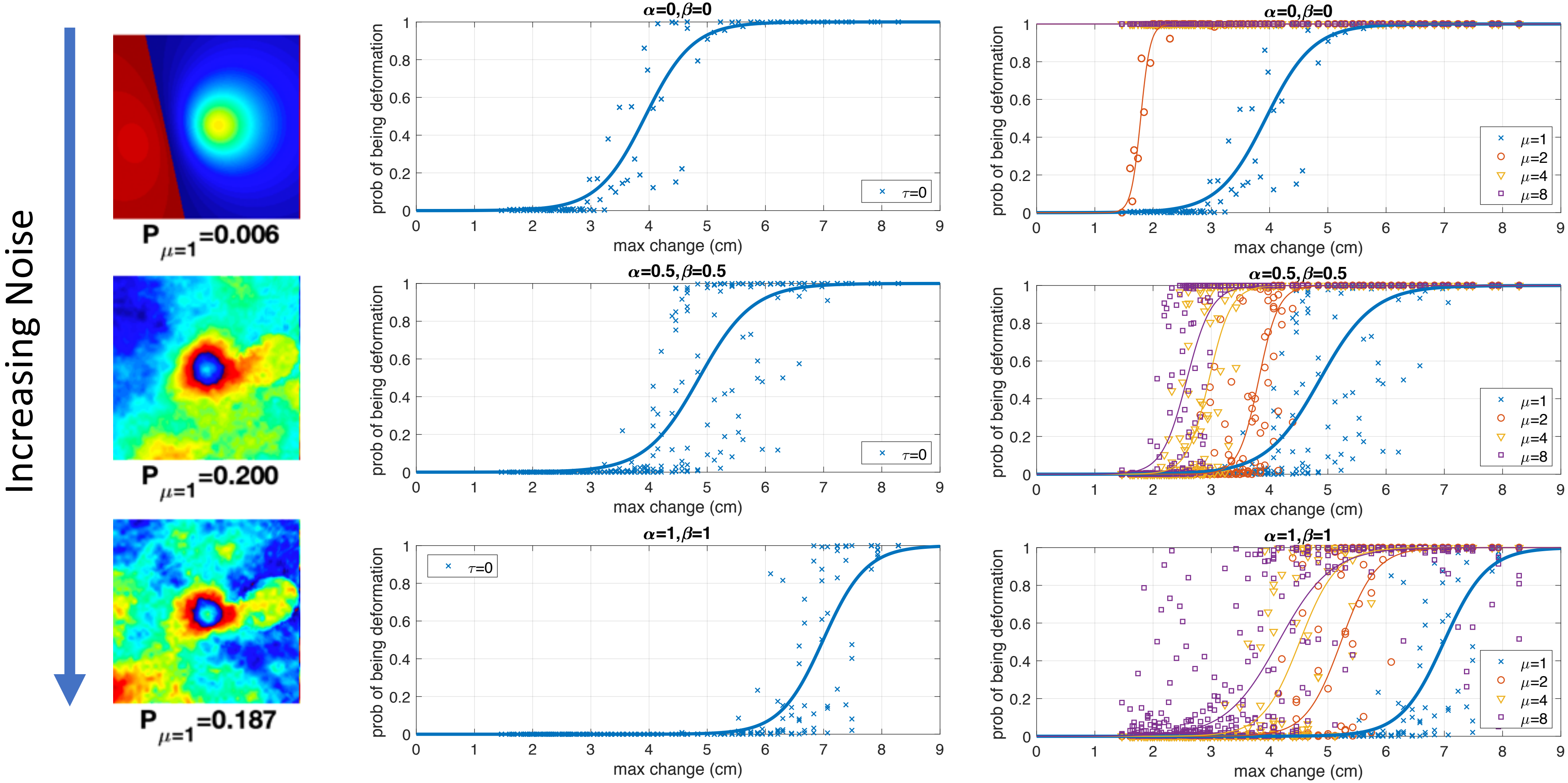

Anantrasirichai et al, in press

Synthetic Data

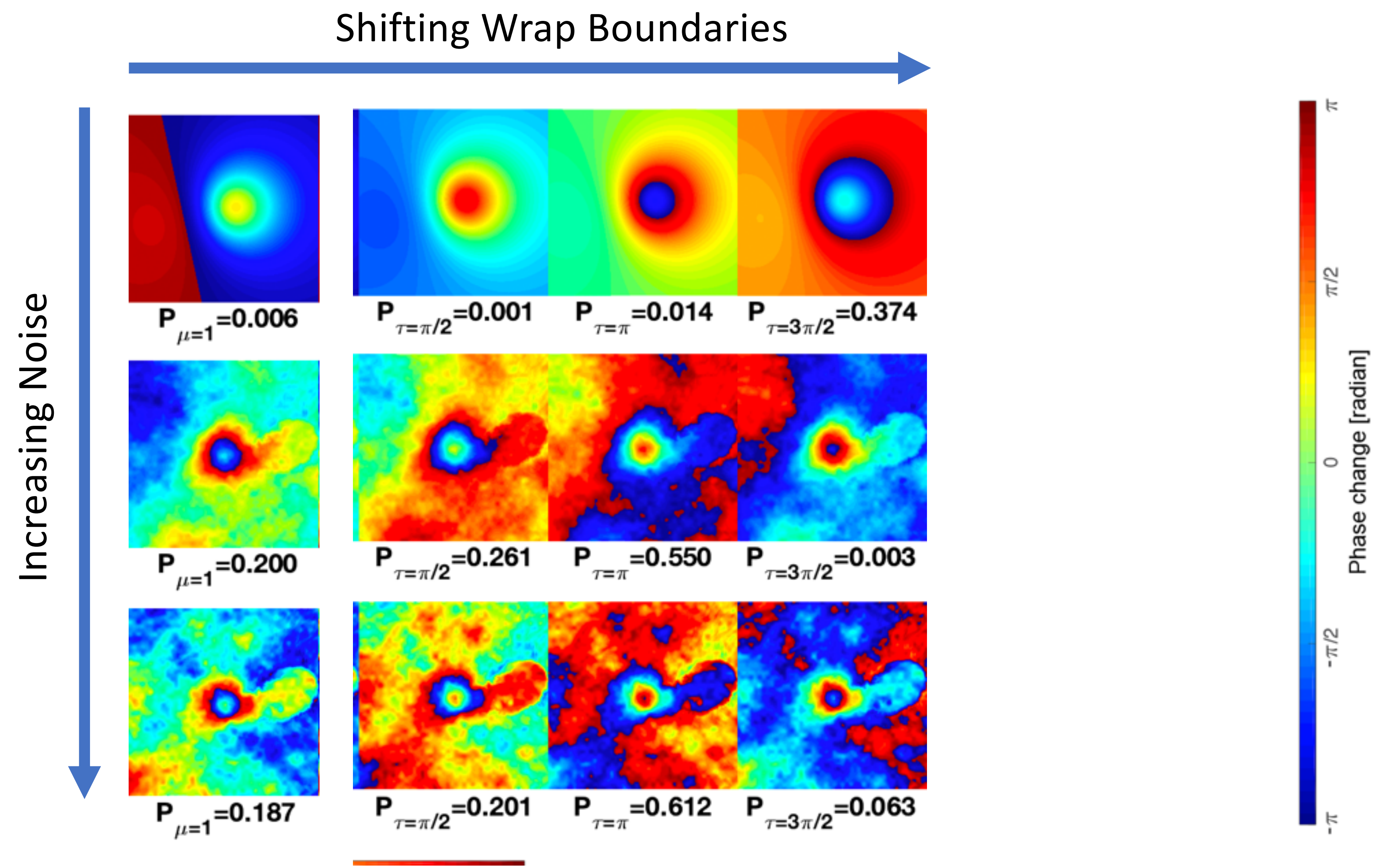

Detection Thresholds: Synthetic Data

Shifting Boundaries (**τ**)

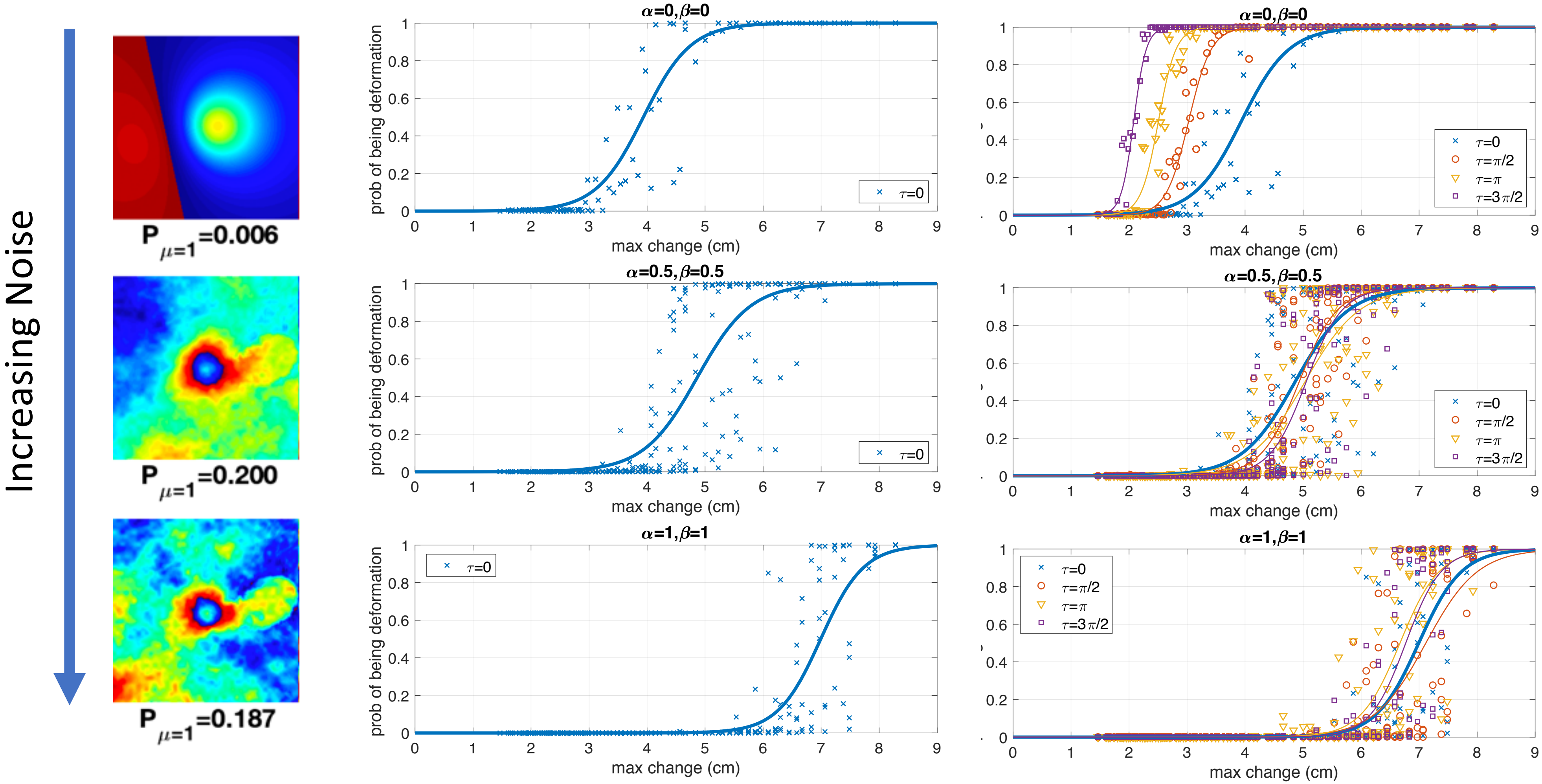

Anantrasirichai et al, in press

Detection Thresholds: Synthetic Data

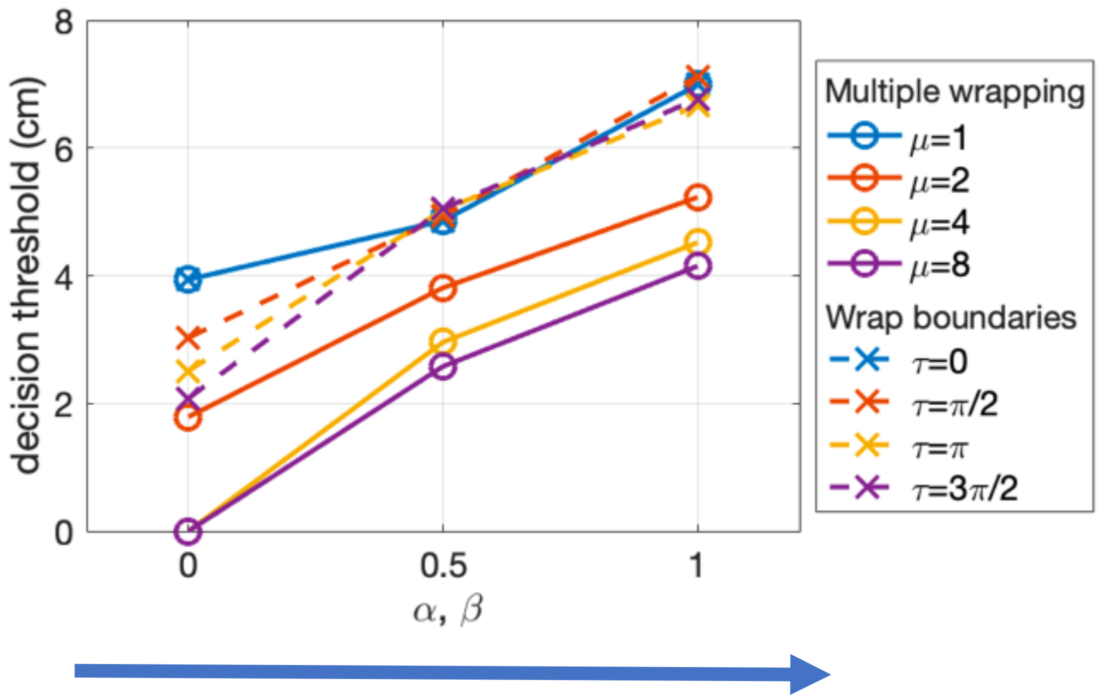

Detection thresholds for wrapped interferograms

- ~ 4cm with no noise.
- >6cm with significant atmospheric noise

Effect of altering wrapping

- Shifting boundaries affects individual cases, but no net effect overall
- Threshold reduced to < 4 cm even in noisy cases by increasing wrap gain.
- But, very high wrap gains cause false positives.

Anantrasirichai et al, in prep

Detecting Slow Deformation

1 fringe in a 12 day interferogram
= 85 cm/yr

4 cm in 4 years of Sentinel-1 data
= 1 cm/yr

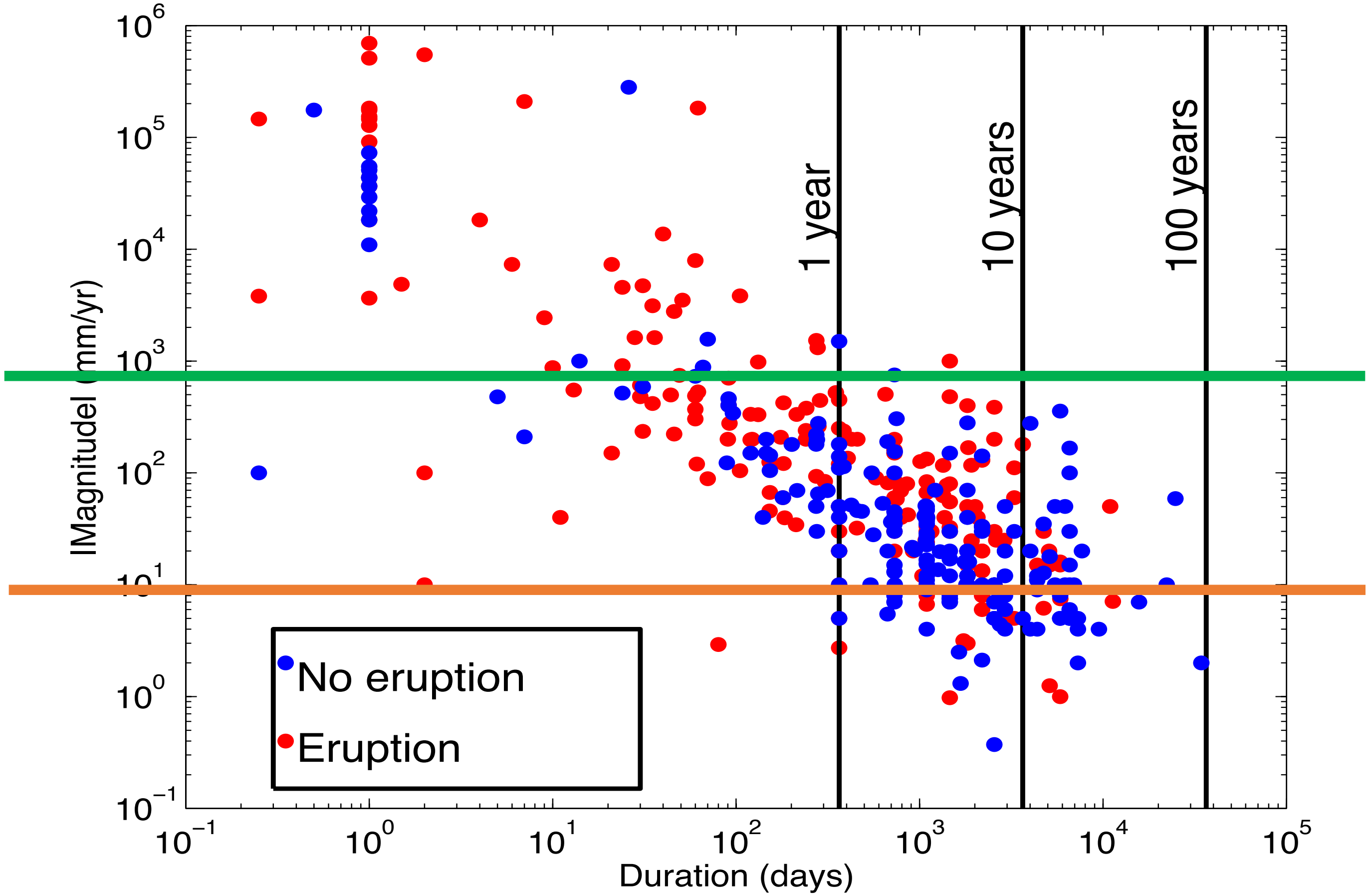

Biggs & Pritchard, 2017

Example 1: Campi Flegrei, Italy

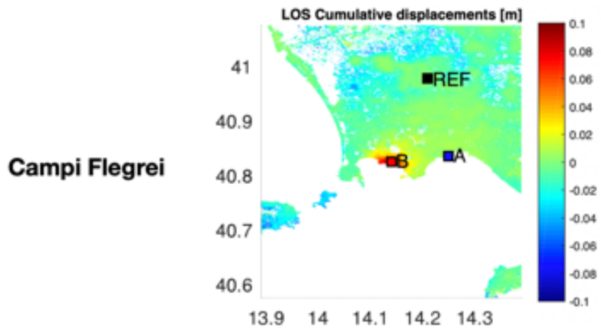

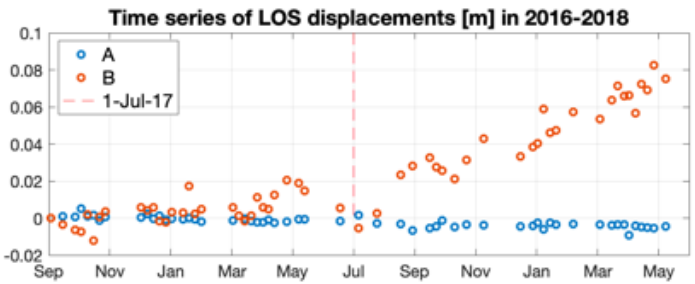

New pulse of uplift started in July 2017, rate of 8.5 cm/yr.

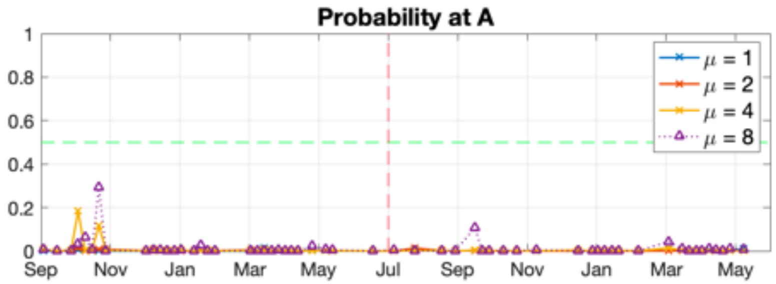

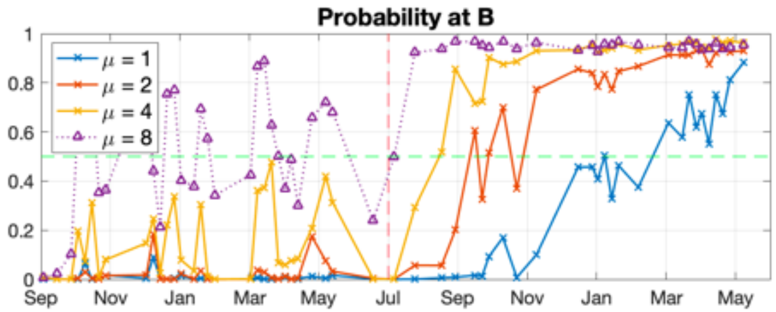

μ=1: detect deformation 7 months after onset (~ 5 cm)

μ=8: 15 false positives before onset of deformation

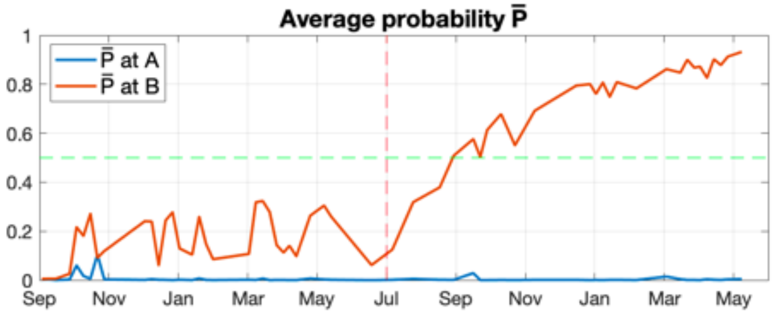

Combined Probability

$$\overline{P} = \frac{1}{N} \sum_{i=0}^{N-1} P_{\mu=2^i}.$$

Detection 2 months after onset

Example 2: Dallol, Ethiopia.

Dallol

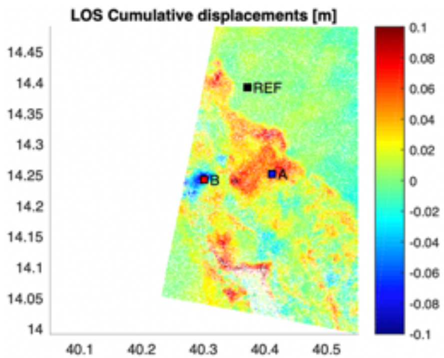

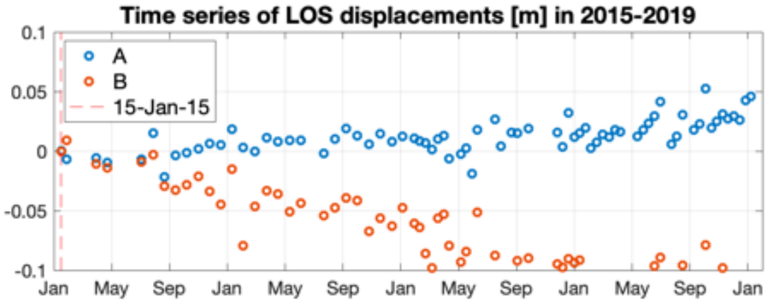

Ongoing subsidence.
Rate of 3.5 cm/yr.

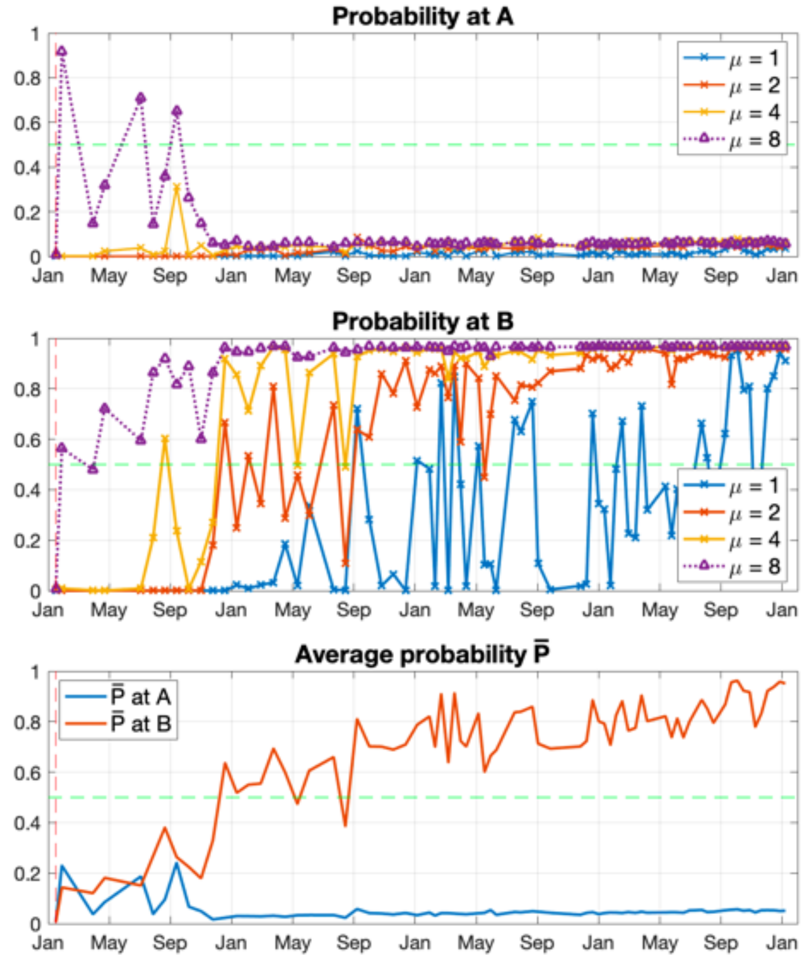

Combined probability detects deformation 11 months after the start of the timeseries.

Performance Metrics

Campi Flegrei

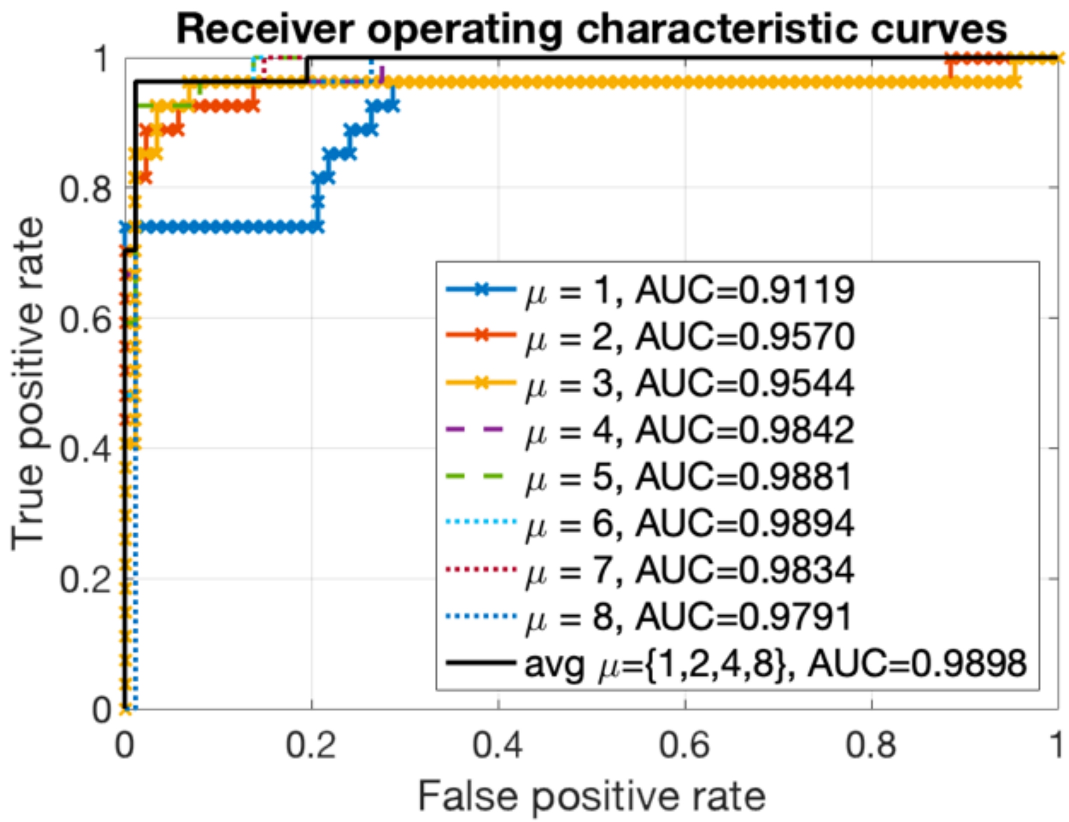

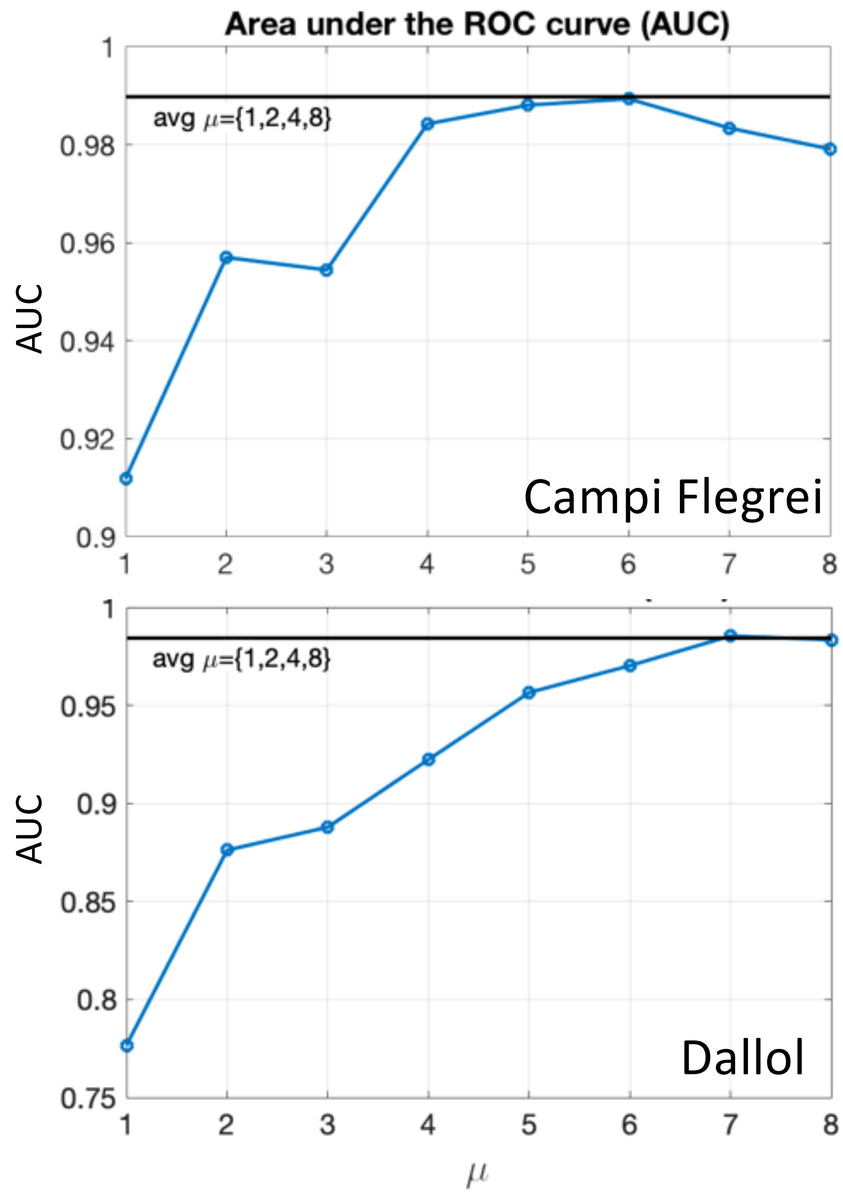

Real-Time Detection (see Fabien's poster)

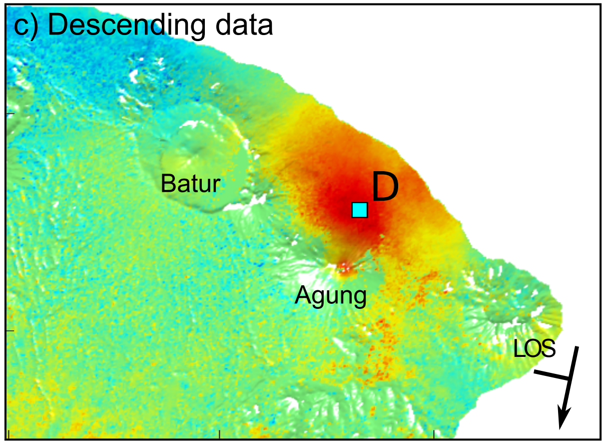

Albino et al, 2019, NComms

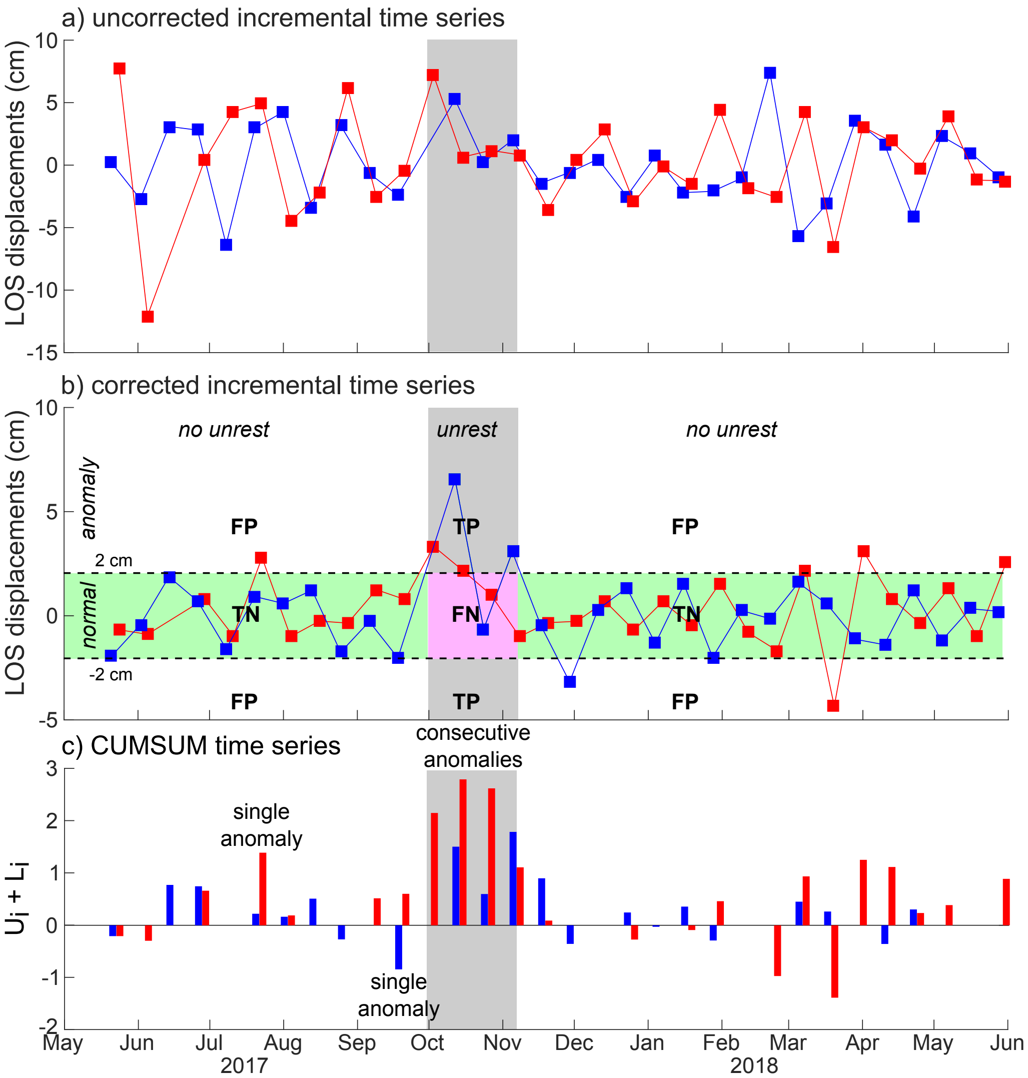

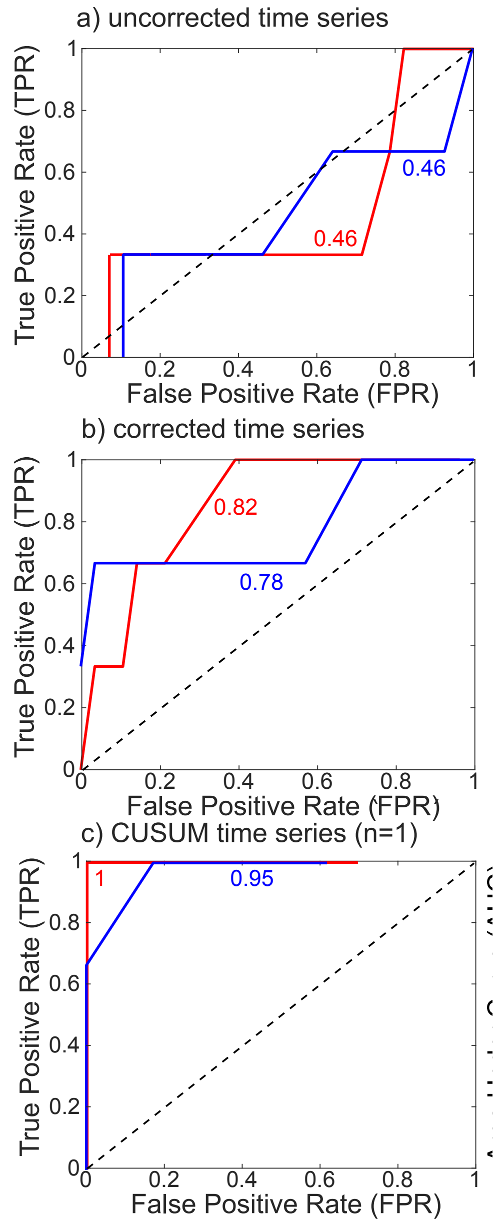

Albino et al, in review, JGR

Conclusions

- **Global datasets** have value for monitoring and understanding magmatic processes.
- **LiCSAR routine processing** producing large data volumes (>200,000 volcano images).
- **Deep learning** framework automatically searches through large volumes of wrapped **InSAR** images to detect rapid **ground deformation** that may be related to **volcanic activity**.
- Problem of **imbalanced training data** was solved using **synthetic examples**, where three major components, i.e. deformation, stratified and turbulent atmosphere.
- **Slow deformation** can be detected using time–series of over-wrapped data.
- May be adaptable to **anthropogenic sources** of deformation

Anantrasirichai, N., Biggs, J., Albino, F., Hill, P. and Bull, D., 2018. Application of Machine Learning to Classification of Volcanic Deformation in Routinely Generated InSAR Data. *Journal of Geophysical Research: Solid Earth*, *123*(8), 6592-6606.
Anantrasirichai, N., Biggs, J., Albino, F., and Bull, D., 2019. A deep learning approach to detecting volcano deformation in satellite imagery using synthetic training data. *Remote Sensing of the Environment. 230, 111179*
Anantrasirichai, N., Biggs, J., Albino, F., and Bull, D., in press. The ability of Convolutional Neural Networks to Detect Slow Ground Deformation in InSAR Timeseries, *Geophysical Research Letters.*

Earth Explorer 10: Harmony

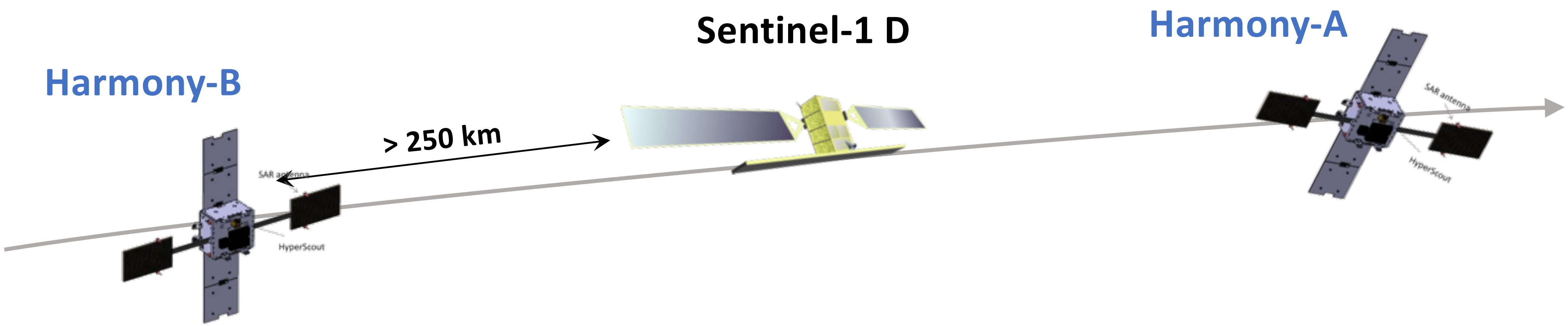

- **Stereo formation**
  - Maximum line-of-sight diversity
  - Best for surface current vectors and 3-D surface deformation

Earth Explorer 10: Harmony

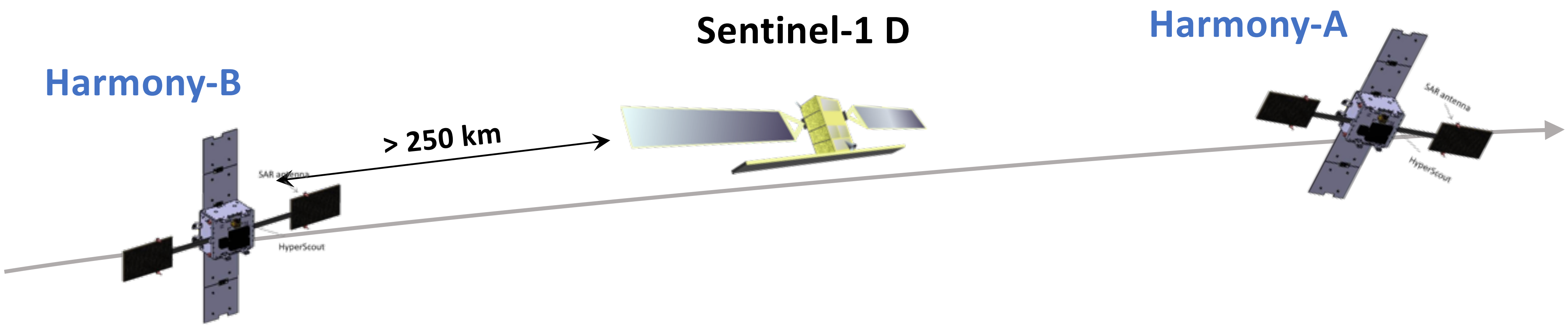

- **XTI formation**
  - Close-formation (TanDEM-X style)
  - Intended for DEM time-series
  - 400 m to 1 km baselines
- **ATI formation**
  - 100 m to 200 m along-track separation

→ Topographic Change at Volcanoes, Landslides, Glaciers etc.

→ 3-D Deformation
3-D Strain Rate

Phase-0 | Phase-A | Phase-BCDE | Exploitation

2020 | 2022 | 2028